Computationally Efficient Method for Calculating Radial Electromagnetic Force of Induction Motor Using Stepping Time-Harmonic Finite Element Analysis

Ji-Hoon Lee[1], Seung-Hun Lee[1], Yun-Jae Won[1], Byeong-Cheol Bae[1], Moo-Hyun Sung[1,2], and Myung-Seop Lim[3]

[1]Department of Automotive Engineering (Automotive-Computer Convergence), Hanyang University, Seoul 04763, South Korea

[2]Vehicle Electrification Research and Development Center, Korea Automotive Technology Institute, Daegu 43011, South Korea

[3]Department of Automotive Engineering, Hanyang University, Seoul 04763, South Korea

Induction motors (IMs) have long been widely used as industrial motors. Although the required characteristics of IMs may vary depending on the application, reducing noise, vibration, and harshness (NVH) is a common requirement across all fields. As demonstrated in multiple studies, the radial electromagnetic force is the most influential factor affecting the vibration characteristics of electric motors. Therefore, analyzing the radial electromagnetic force is essential for enhancing the vibration performance of electric motors. However, finite element analysis (FEA) of IMs requires considerable computation time, as it must be conducted as a transient analysis. In this article, stepping time-harmonic FEA is proposed for the fast calculation of the radial electromagnetic force in IMs. Unlike conventional time-harmonic FEA, the proposed method incorporates mechanical and electrical rotation of the IM in the analysis. The proposed method was used to obtain the air-gap flux density over one electrical period, and the radial electromagnetic force density was calculated using Maxwell stress tensor (MST). The spatial and temporal orders of the radial electromagnetic force density were analyzed using 2-D fast Fourier transform (FFT), and good agreement was confirmed between the proposed method and the 2-D transient FEA. The proposed method significantly reduces the computation time required for calculating the radial electromagnetic force density compared to 2-D transient FEA. Therefore, it was confirmed that the proposed method enables rapid computation of the radial electromagnetic force density in the IM while ensuring a high level of accuracy.

Index Terms— **Electromagnetic force, induction motor (IM), stepping time-harmonic finite element analysis.**

I. Introduction

INDUCTION motors (IMs) have long been widely used as industrial motors. They have been used in applications such as fans, pumps, railway systems, compressors, and conveyors. With the recent rise of environmental concerns, the demand for electric vehicles (EVs) has increased, and IMs are being actively studied as traction motors for EVs. Although the required characteristics of IMs may vary depending on the application, reducing noise, vibration, and harshness (NVH) is a common requirement across all fields. As demonstrated in multiple studies, the radial electromagnetic force is the most influential factor affecting the vibration characteristics of electric motors. Therefore, analyzing the radial electromagnetic force is essential for enhancing the vibration performance of electric motors.

However, finite element analysis (FEA) of IMs requires considerable computation time, as it must be conducted as a transient analysis. As the rotational speed of IMs increases and slip decreases, the computation time grows exponentially. Even though the analysis of IMs through transient FEA is accurate, this drawback makes it difficult to perform such analyses. To overcome the issue of extended computation times in IM analysis, several studies have been conducted. A method for analytically evaluating iron losses caused by PWM, considering supply harmonics of the inverter and slot harmonics, was proposed in [1]. In [2], a 2-D subdomain model was proposed to analyze the electromagnetic characteristics of squirrel cage IM by considering the rotor slotting effect and the skin effect in rotor conductor bars. In [3], a general analytical model was proposed for analyzing the inductance and torque of IMs. Zhang et al. [1], Devillers et al. [2], and Marfoli et al. [3] all reduced computation time compared to transient FEA by employing analytical methods. There are also cases where computation time has been reduced by using time-harmonic FEA. AC copper loss in the stator of a motor with hairpin windings is calculated using time-harmonic FEA in [4]. To calculate the eddy current losses in solid rotor IMs, Räisänen et al. [5] proposed a time-harmonic analytical model. In [6], time-harmonic FEA was performed using the virtual blocked rotor method and the frozen permeability method, and the results were used as initial conditions for transient FEA to reduce computation time. A method for calculating the force in linear IMs, along with a way to account for the magnetic non-linearity of the core, was proposed in [7]. Ling et al. [8] calculated the parameters of the single-phase equivalent circuit of an IM using time-harmonic FEA. Several studies have been conducted to accelerate vibration analysis of electric motors. In [9], electromagnetic force and vibration analysis of a PMSM was carried out using an analytical

Received 19 July 2025; revised 10 December 2025; accepted 12 January 2026. Date of publication 19 January 2026; date of current version 13 July 2026. Corresponding author: M.-S. Lim (e-mail: myungseop@hanyang.ac.kr).

Color versions of one or more figures in this article are available at https://doi.org/10.1109/TMAG.2026.3655404.

Digital Object Identifier 10.1109/TMAG.2026.3655404

method to reduce analysis time, which was then incorporated into the optimal design process. Hybrid evaluation method was proposed in [10] for rapid and accurate analysis of electromagnetic force and vibration caused by high-frequency components resulting from pulsewidth modulation. In [11], the electromagnetic forces generated by the PWM inverter in an IPMSM were rapidly computed using a small-signal time-harmonic FEA approach. It demonstrated significantly reduced computation time compared to transient FEA while maintaining high accuracy. Although [9], [10], and [11] pursue rapid electromagnetic force and vibration analysis for PMSMs, IMs also require an equally efficient analysis approach. However, no method has yet been proposed for the rapid evaluation of radial electromagnetic forces in IMs.

In this article, a stepping time-harmonic FEA is proposed for the fast calculation of the radial electromagnetic force in IMs. Unlike conventional time-harmonic FEA, the proposed method incorporates mechanical and electrical rotation of the IM in the analysis. Through the proposed method, the air-gap flux density over one electrical cycle can be obtained, and the radial electromagnetic force density can be calculated using Maxwell stress tensor (MST). A 2-D fast Fourier transform (FFT) is applied to the radial electromagnetic force density to analyze its spatial and temporal orders. For validation, vibration analysis was performed, and the radial displacement was compared with experimental measurements. By comparing the experimental results with those obtained from the proposed method, good agreement was observed, confirming the effectiveness of the stepping time-harmonic FEA.

This article is organized as follows. In Section II, two FEA methods for analyzing IMs, namely, transient FEA and time-harmonic FEA, are introduced and the characteristics of each method are discussed. Section III describes the stepping time-harmonic FEA method proposed in this article. Section IV describes the calculation of the radial electromagnetic force density using FEA and its application to motor vibration analysis. Section V compares the radial electromagnetic force densities from the proposed method and 2-D transient FEA and validates the vibration analyses against experimental results. The conclusion of this article is summarized in Section VI.

II. FEA for IM

This section discusses two analysis methods for IMs commonly used in FEA. In FEA, IMs are analyzed using either transient FEA or time-harmonic FEA. In 2-D FEA, the governing equations for the two analysis methods are given in the following equations [12], [13]:

$$\frac{\partial}{\partial x}\left(\frac{1}{\mu}\frac{\partial A_z}{\partial x}\right)+\frac{\partial}{\partial y}\left(\frac{1}{\mu}\frac{\partial A_z}{\partial y}\right)=-J_o+\sigma\frac{\partial A_z}{\partial t} \quad (1)$$

$$\frac{\partial}{\partial x}\left(\frac{1}{\mu}\frac{\partial A_z}{\partial x}\right)+\frac{\partial}{\partial y}\left(\frac{1}{\mu}\frac{\partial A_z}{\partial y}\right)=-J_o+j\omega\sigma A_z \quad (2)$$

where A_z is the magnetic vector potential in the z-axis, μ is the permeability, J_o is the source current density, ω is the angular frequency, and σ is the conductivity. An example of the application of the two analysis methods is shown in Fig. 1. In Fig. 1(a), the current and torque waveforms obtained

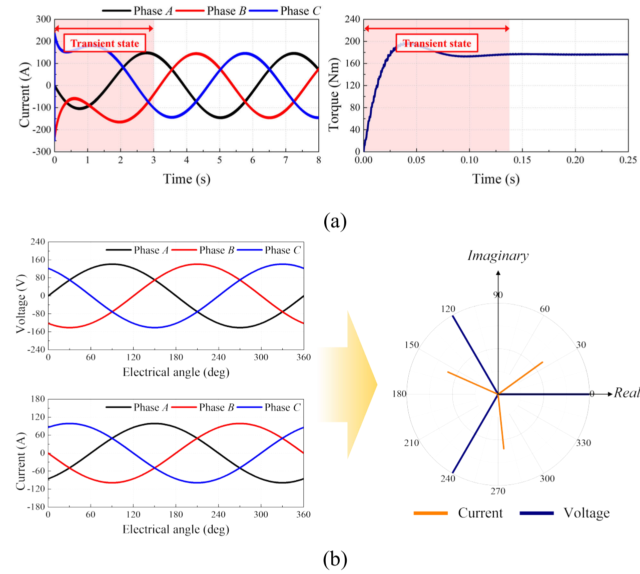

Fig. 1. Features of each analysis method. (a) Transient FEA and (b) time-harmonic FEA.

from the transient FEA exhibit a transient state, as indicated by the red-shaded region. It can be observed that a transient state appears for a certain period and gradually converges to a steady state. In electrical machine design, the steady-state values following the transient period are required in most cases. Accordingly, since IMs require a certain period for the transient state to reach a steady state, the overall analysis time tends to be extended. Time-harmonic FEA assumes that the time variation of the field is sinusoidal, as expressed in (2). That is, as shown in Fig. 1(b), time-harmonic FEA solves the governing equation in the complex plane, and all physical quantities are consequently represented as complex values. Since the field variation is assumed to be sinusoidal, the method is less accurate but requires only a single-step analysis, which leads to faster computation time.

When high accuracy is required, transient FEA is used, as shown in Fig. 2. The computation time for transient FEA of IMs can increase exponentially in some cases. When deriving the steady-state characteristics of IMs, data for one period of the slip frequency is needed. The slip frequency is determined by the slip, which is the ratio of the speed difference between the rotating magnetic field of the stator and the rotor, and as the slip decreases, the slip frequency also decreases. As the slip frequency decreases, the time required for one cycle of the slip frequency becomes longer, which consequently leads to an increase in total analysis time. In some cases, an increase in the rotational speed of an IM requires a corresponding increase in the speed of the rotating magnetic field produced by the stator. The speed of the rotating magnetic field of the stator, referred to as the synchronous speed, is calculated as follows:

$$n=\frac{120f}{p} \quad (3)$$

where n is the synchronous speed of the rotating magnetic field, f is the stator source frequency, and p is the number of poles. As shown in (3), increasing the synchronous

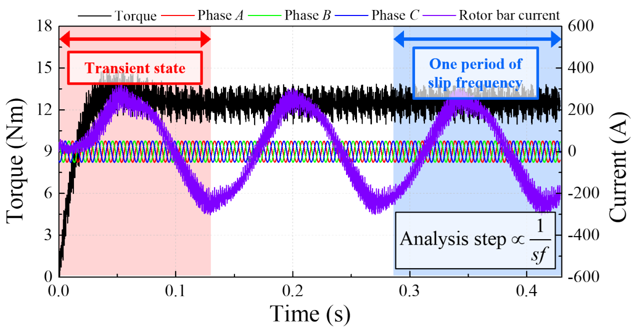

Fig. 2. Transient behavior and slip characteristics affecting analysis time in IMs when using transient FEA.

speed requires an increase in the stator source frequency. This implies that the period of the stator becomes shorter. In other words, as the speed increases and the slip decreases, numerous stator source periods exist within a single rotor source period. In addition, when considering the transient state, the analysis may not converge within a single rotor source period. Therefore, in most cases, analysis over multiple rotor periods is required rather than a single period. In this article, the analysis step for the IM in transient FEA is calculated as follows:

$$N_{\text{FEA}} = \frac{(1/sf)}{\left(1/\left(\omega_m \times pp + sf\right)/N_{\text{step}}\right)} \times N_{\text{period}} + 1 \quad (4)$$

where N_{FEA} is the total number of analysis steps for transient FEA, sf is the slip frequency, ω_m is the rotational speed of the rotor, pp is the pole pair, N_{step} is the number of samplings in one stator period, and N_{period} is the number of rotor source periods for steady state. Although N_{period} may need to be larger depending on the analyzed load condition, a value of 3 was used in this article.

III. Stepping Time-Harmonic FEA

In this section, the stepping time-harmonic FEA method proposed in this article is described. Stepping time-harmonic FEA is a method developed from the idea of combining the fast computation time of time-harmonic FEA with the ability to simulate rotational behavior, as in transient FEA. Conventional time-harmonic FEA is based on a single-step analysis and therefore does not account for the stepwise mechanical rotation modeled in transient FEA, nor the phase angle of the stator current. To obtain the radial electromagnetic force, the air-gap flux density must be evaluated over both time and space, but in this method, it can be derived for only one step at a time.

The key feature of the stepping time-harmonic FEA lies in its ability to incorporate mechanical and electrical rotation, which are not considered in conventional time-harmonic FEA. The information regarding mechanical and electrical rotation is shown in Fig. 3. Mechanical rotation θ_m is implemented by updating the rotor position at each analysis step. Similarly, electrical rotation θ_e is implemented by incorporating the phase shift of the current at each analysis step. The method is referred to as stepping time-harmonic FEA because it involves both mechanical and electrical rotation at each step.

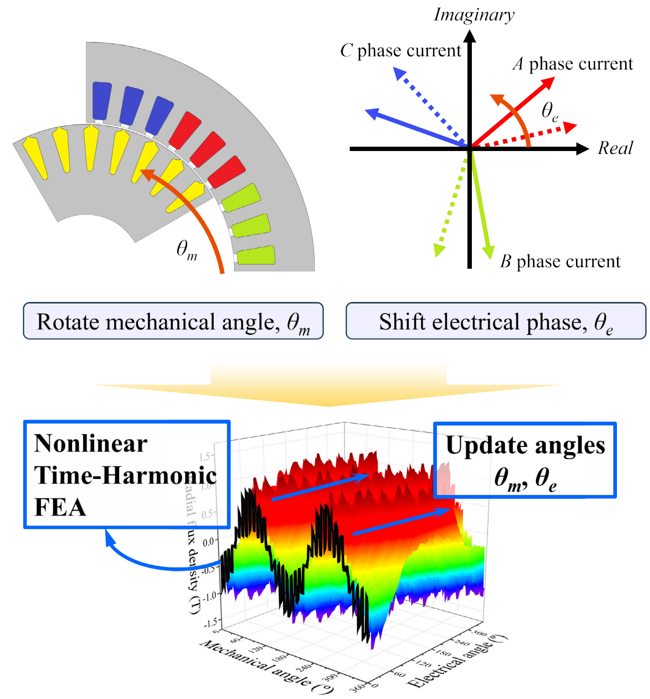

Fig. 3. Information on mechanical angle rotation and electrical phase shift.

By incorporating both rotations in the analysis, the air-gap flux density as a function of time and space can be obtained, as shown in Fig. 3. In conventional time-harmonic FEA, only the air-gap flux density for a single time step, indicated by the black line in Fig. 3, can be obtained. However, by using the proposed method, it is possible to obtain the air-gap flux density to calculate the radial electromagnetic force.

The analysis process of the stepping time-harmonic FEA is illustrated in Fig. 4. First, the conditions required for the analysis are determined, including the magnitude of the stator current, slip frequency, and the number of samples for one electrical period. Then, the mechanical rotation angle and the electrical phase for each analysis step are calculated for stepping. Next, the non-linear time-harmonic FEA is performed by inputting the analysis conditions, including the magnitude of the current, slip frequency, mechanical angle, and electrical phase. The process is repeated over one period of slip frequency by updating the mechanical angle and electrical phase at each step. Once the analysis of one slip frequency is completed, the air-gap flux density at each step is obtained. Using the air-gap flux density, the radial electromagnetic force is calculated, and its spatial and temporal orders are extracted through 2-D FFT, concluding the analysis process.

In transient FEA, the number of analysis steps is determined, as shown in (4). As previously explained, the number of analysis steps increases exponentially with higher speed and lower slip. In contrast, the number of analysis steps in stepping time-harmonic FEA is determined solely by N_{step}, the number of samplings per one electrical period. This enables a substantial reduction in the computation time for analyzing IMs. For example, in a four-pole IM with a rotational speed of 3000 r/min, a slip frequency of 0.5 Hz, and an N_{step} of 60,

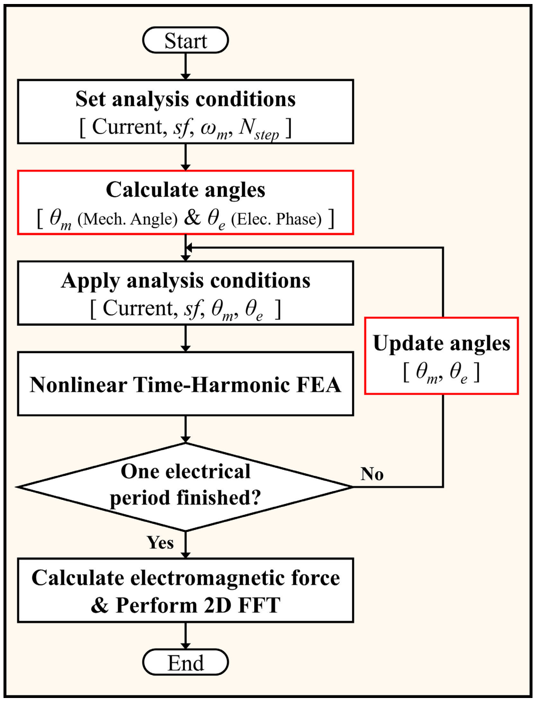

Fig. 4. Analysis flowchart of stepping time-harmonic FEA.

transient FEA requires 36 181 analysis steps, whereas stepping time-harmonic FEA requires only 60 steps.

IV. Vibration Analysis

This section explains the method for deriving the radial electromagnetic force of IMs and performing the corresponding vibration analysis. The analysis procedure is illustrated in Fig. 5. For vibration analysis, both electromagnetic and mechanical analyses are performed. In the electromagnetic analysis, the air-gap flux density under load conditions of the IM is obtained to derive the radial electromagnetic force. The radial electromagnetic force is calculated using MST, as follows:

$$P_r = \frac{B_r^2 - B_t^2}{2\mu_0} \tag{5}$$

where P_r is the radial electromagnetic force density, B_r is the radial flux density, B_t is the tangential flux density, and μ_0 is the permeability in vacuum. The radial electromagnetic force is calculated as a concentrated force applied to each tooth of the stator [14]. In the mechanical analysis, the natural frequencies of each mode of the stator are obtained through modal analysis. Finally, the radial displacement of the stator is calculated using mode superposition.

V. Validation

This section evaluates the effectiveness of the proposed method by comparing it with 2-D transient FEA and verifies its validity through comparison with experimental results. The IM used for validation of the proposed method is shown in Fig. 6, and its specifications are listed in Table I. A 37 kW IE4 grade industrial IM was used in this study. The rotor consists of an aluminum structure employing a double-cage design. In the

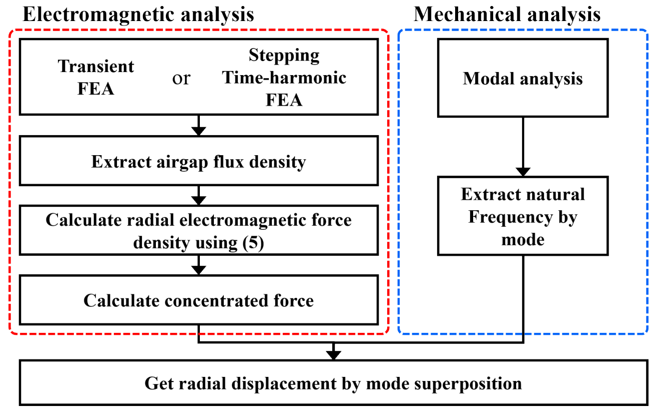

Fig. 5. Analysis flowchart of vibration analysis.

TABLE I
Specifications of IM

Item	Unit	Value
Number of poles	-	4
Number of stator slots	-	48
Number of rotor bars	-	40
Supply frequency	Hz	60
Rated power	kW	37
Rated torque	Nm	190
Rated speed	rpm	1785
Rated current	Arms	70
Rated slip	%	0.83

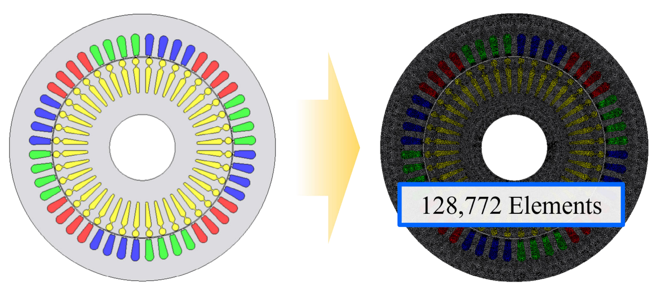

Fig. 6. Configuration of target IM.

TABLE II
Operating Points Used for Analysis

Slip	Unit	Notes
(OP 1) 0.42	%	50% of rated point
(OP 2) 0.83	%	Rated point
(OP 3) 1.67	%	200% of rated point

FEA modeling of the IM, a total of 128 772 mesh elements were generated, as shown in Fig. 6.

First, a comparison is made between the radial electromagnetic force densities obtained from the proposed method and the 2-D transient FEA to confirm their consistency. Validation was conducted at three operation points, including the rated load point of the IM, and these operating points are listed in Table II. Fig. 7 presents the air-gap flux density waveforms in the radial and tangential directions according to the mechanical angle and electrical phase at rated load points. The waveforms confirm a high level of agreement in air-gap flux density between 2-D transient FEA and the stepping time-harmonic

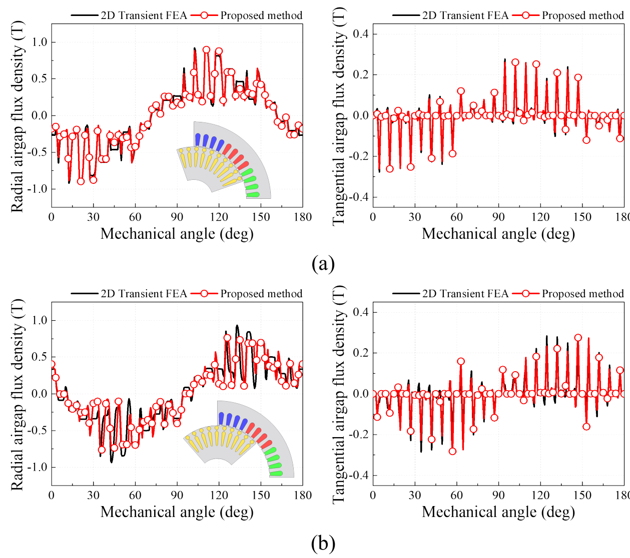

Fig. 7. Comparison of air-gap flux density between 2-D transient FEA and stepping time-harmonic FEA at rated load. (a) $\theta_m = 19.35$ (mdeg) and $\theta_e = 36$ (edeg). (b) $\theta_m = 41.17$ (mdeg) and $\theta_e = 80$ (edeg).

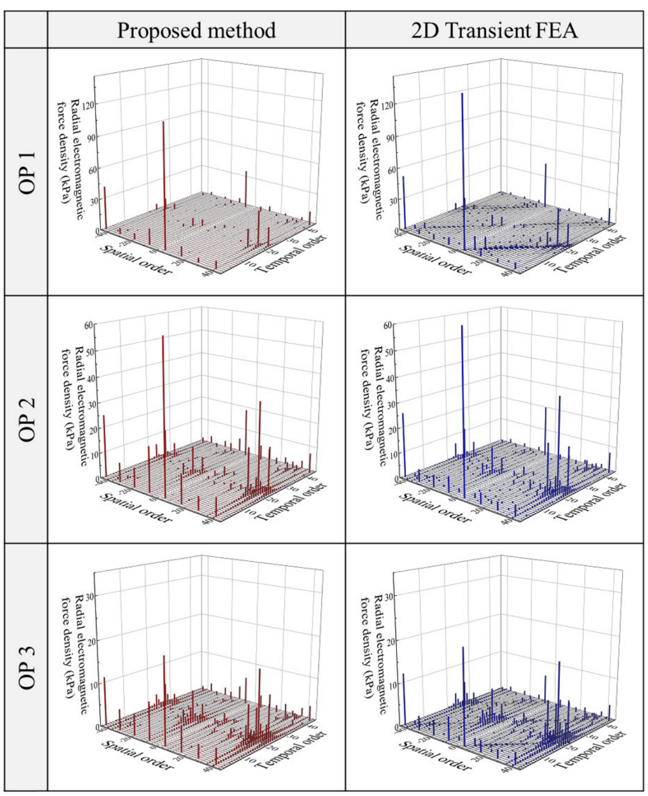

Fig. 8. Spectrum of radial electromagnetic force density at each operating point.

FEA. The radial electromagnetic force calculated from the air-gap flux density over time and space using (5) is analyzed by 2-D FFT to extract its spatial and temporal orders, as shown in Fig. 8. Among the spectrum of the radial electromagnetic force density in Fig. 8, the spatial orders corresponding to the second temporal order are shown in Fig. 9. It can be observed that the fourth spatial order, corresponding to the pole number, is the most dominant component. At the fourth spatial order, the error for OP 1 is 17.09%, the error for

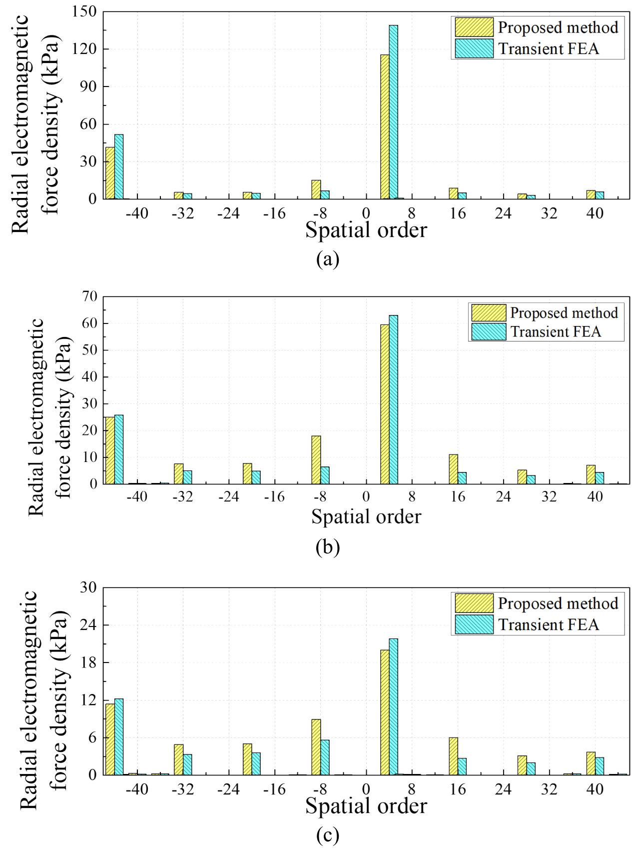

Fig. 9. Comparison of spatial order at second temporal order between 2-D transient FEA and stepping time-harmonic FEA. (a) OP 1, (b) OP 2, and (c) OP 3.

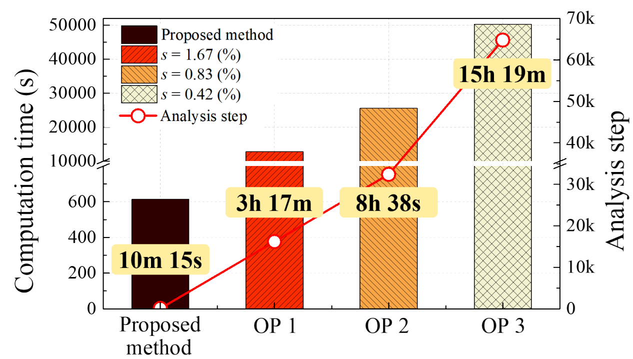

Fig. 10. Comparison of computation time between 2-D transient FEA and stepping time-harmonic FEA.

OP 2 is 5.58%, and the error for OP 3 is 8.39%. Although there are some differences depending on the operating point, the dominant orders remain the same, and the variations are within an acceptable range. Fig. 10 shows the computation time and the number of analysis steps for each method. For the electromagnetic analysis, the finite element software JMAG was used, and the computing system employed was the 14th Gen Intel[1] Core[2] i7-14700K. While 2-D transient FEA typically requires several hours of computation time,

[1]Registered trademark.
[2]Trademarked.

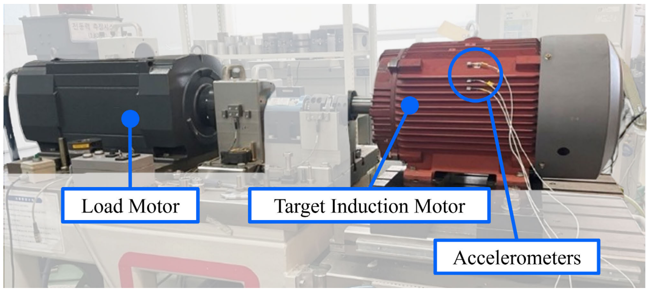

Fig. 11. Vibration experimental setup.

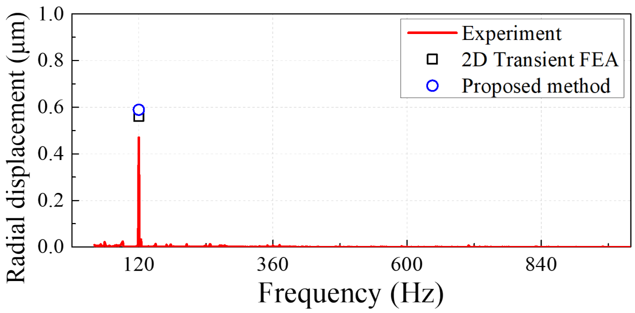

Fig. 12. Comparison of radial displacement under rated load conditions.

the stepping time-harmonic FEA completes the analysis in approximately 10 min. The proposed method demonstrated its effectiveness by showing minimal difference from the 2-D transient FEA in deriving the radial electromagnetic force of the IM while significantly reducing the computation time.

Next, vibration analysis was conducted as described in Section IV. At the rated load operating point, the radial electromagnetic forces obtained from stepping time-harmonic FEA and 2-D transient FEA were used and compared with experimental results. The assembled experimental setup is shown in Fig. 11. During operation at the rated load, an accelerometer attached to the housing of the IM measured acceleration, from which the radial displacement was calculated. Fig. 12 shows the radial displacement according to frequency. The largest displacement was observed at 120 Hz, corresponding to the second temporal harmonic, and good agreement was confirmed between the experimental results and each analysis.

VI. Conclusion

In this article, a stepping time-harmonic FEA method for the rapid calculation of the radial electromagnetic force in IMs is proposed. The non-linear time-harmonic FEA was performed, while the IM was rotating both mechanically and electrically. The proposed method was used to obtain the air-gap flux density over one electrical period, and the radial electromagnetic force density was calculated using MST. The spatial and temporal orders of the radial electromagnetic force density were analyzed using 2-D FFT, and good agreement was confirmed between the proposed method and the 2-D transient FEA. To validate the results, vibration analysis was performed, and the calculated radial displacements showed good agreement with the experimental measurements. The proposed method significantly reduces the computation time required for calculating the radial electromagnetic force density compared to the 2-D transient FEA. Therefore, it was confirmed that the proposed method enables rapid computation of the radial electromagnetic force density in the IM while ensuring a high level of accuracy.

Acknowledgment

This work was supported by the Korea Institute of Energy Technology Evaluation and Planning (KETEP) grant funded by the Korea government (MOTIE) (No. RS-2023-00232593, Development of common base technology for medium power industrial motors).

References

[1] D. Zhang, T. Liu, H. Zhao, and T. Wu, "An analytical iron loss calculation model of inverter-fed induction motors considering supply and slot harmonics," *IEEE Trans. Ind. Electron.*, vol. 66, no. 12, pp. 9194–9204, Dec. 2019.

[2] E. Devillers, J. L. Besnerais, T. Lubin, M. Hecquet, and J.-P. Lecointe, "An improved 2-D subdomain model of squirrel-cage induction machine including winding and slotting harmonics at steady state," *IEEE Trans. Magn.*, vol. 54, no. 2, pp. 1–12, Feb. 2018.

[3] A. Marfoli, L. Papini, P. Bolognesi, and C. Gerada, "An analytical-numerical approach to model and analyse squirrel cage induction motors," *IEEE Trans. Energy Convers.*, vol. 36, no. 1, pp. 421–430, Mar. 2021.

[4] A. Tessarolo, F. Agnolet, F. Luise, and M. Mezzarobba, "Use of time-harmonic finite-element analysis to compute stator winding eddy-current losses due to rotor motion in surface permanent-magnet machines," *IEEE Trans. Energy Convers.*, vol. 27, no. 3, pp. 670–679, Sep. 2012.

[5] V. Räisänen, S. Suuriniemi, S. Kurz, and L. Kettunen, "Rapid computation of harmonic eddy-current losses in high-speed solid-rotor induction machines," *IEEE Trans. Energy Convers.*, vol. 28, no. 3, pp. 782–790, Sep. 2013.

[6] H. Chen, H. N. Koti, N. A. O. Demerdash, K. M. Rahman, and Y. Sun, "Fast steady-state analysis in time-stepping finite-element simulation of induction motors based on virtual blocked rotor techniques," *IEEE Trans. Ind. Appl.*, vol. 56, no. 4, pp. 3731–3743, Jul. 2020.

[7] A. Z. Bazghaleh and E. F. Choolabi, "A new approach for non-linear time-harmonic FEM-based analysis of single-sided linear induction motor incorporated with a new accurate method of force calculation," *IEEE Trans. Magn.*, vol. 57, no. 2, pp. 1–9, Feb. 2021.

[8] Z. Ling, L. Zhou, S. Guo, and Y. Zhang, "Equivalent circuit parameters calculation of induction motor by finite element analysis," *IEEE Trans. Magn.*, vol. 50, no. 2, pp. 833–836, Feb. 2014.

[9] L. Yao, J.-X. Shen, Y. Wang, and D. Shi, "Fast prediction and staged optimization of electromagnetic vibration in permanent magnet synchronous motor," *IEEE Trans. Ind. Electron.*, vol. 71, no. 1, pp. 115–125, Jan. 2024.

[10] Y. Lu, J. Li, and K. Yang, "A hybrid calculation method of electromagnetic vibration for electrical machines considering high-frequency current harmonics," *IEEE Trans. Ind. Electron.*, vol. 69, no. 10, pp. 10385–10395, Oct. 2022.

[11] S. Zhu, J. Lu, and F. Zeng, "Fast calculation of electromagnetic forces in IPMSMs under PWM VSI supply based on small-signal time-harmonic finite element method," *CES Trans. Electr. Mach. Syst.*, vol. 6, no. 1, pp. 67–76, Mar. 2022.

[12] D.-J. Kim, D.-K. Hong, J.-H. Choi, Y.-D. Chun, B.-C. Woo, and D.-H. Koo, "An analytical approach for a high speed and high efficiency induction motor considering magnetic and mechanical problems," *IEEE Trans. Magn.*, vol. 49, no. 5, pp. 2319–2322, May 2013.

[13] S. J. Salon, *Finite Element Analysis of Electrical Machines*. Norwell, MA, USA: Kluwer, 1995.

[14] J.-H. Kim, S.-H. Park, J.-Y. Ryu, and M.-S. Lim, "Comparative study of vibration on 10-pole 12-slot and 14-pole 12-slot PMSM considering tooth modulation effect," *IEEE Trans. Ind. Electron.*, vol. 70, no. 4, pp. 4007–4017, Apr. 2023.